Accelerated life tests for prognostic and health management of MEMS devices

Haithem Skima, Kamal Medjaher, and Noureddine Zerhouni

FEMTO-ST Institute, AS2M department, Franche-Comté University/CNRS/ENSMM
24 rue Alain Savary, 25000 Besançon, France.
haithem.skima@femto-st.fr, kamal.medjaher@ens2m.fr

ABSTRACT

Microelectromechanical systems (MEMS) offer numerous applications thanks to their miniaturization, low power consumption and tight integration with control and sense electronics. They are used in automotive, biomedical, aerospace and communication technologies to achieve different functions in sensing, actuating and controlling. However, these microsystems are subject to degradations and failure mechanisms which occur during their operation and impact their performances and consequently the performances of the systems in which they are used. These failures are due to different influence factors such as temperature, humidity, etc. The reliability of MEMS is then considered as a major obstacle for their development. In this context, it is necessary to continuously monitor them to assess their health status, detect abrupt faults, diagnose the causes of the faults, anticipate incipient degradations which may lead to complete failures and take appropriate decisions to avoid abnormal situations or negative outcomes. These tasks can be performed within Prognostics and Health Management (PHM) framework.

This paper presents a hybrid PHM method based on physical and data-driven models and applied to a microgripper. The MEMS is first modeled in a form of differential equations. In parallel, accelerated life tests are performed to derive its degradation model from the acquired data. The nominal behavior and the degradation models are then combined and used to monitor the microgripper, assess its health state and estimate its Remaining Useful Life (RUL).

1. INTRODUCTION

Current maintenance strategies have progressed from breakdown maintenance, to preventive maintenance, then to condition based maintenance CBM (Aiwina, Sheng, Andy, & Joseph, 2009).

CBM is a maintenance program that recommends maintenance decision based on the information collected through condition monitoring. It consists of three main steps: data acquisition, data processing and maintenance decision making. The key process of CBM is Prognostic and Health Management (PHM), an approach that estimates the Remaining Useful Life (RUL) of systems based on their current health state and their future operating conditions. Prognostic approaches can be categorized into three classes, namely model-based (also called physics-based approach), data-driven and hybrid prognostic approaches (Jay et al., 2014).

Model-based prognostics deal with the prediction of the RUL of components by using mathematical or physical models to describe the degradation phenomena. Data-driven prognostics aim at transforming sensory data into relevant models of the degradation behavior (Medjaher, Tobon-Mejia, & Zerhouni, 2012). In general, hybrid prognostic approach benefits from both categories to overcome their drawbacks, for example, (Hansen, Hall, & Kurtz, 1995) proposed an approach which fuses the outputs from model-based and data-driven approaches. Prognostic results obtained from this approach are claimed to be more reliable and accurate (Jay et al., 2014).

PHM approaches can be applied to MEMS to improve the reliability and availability of systems in which they are utilized, to avoid failures and to reduce maintenance costs. However, the miniaturization of these microsystems makes the implementation of PHM approaches more specific.

This paper presents a hybrid prognostic method applied to microgripper MEMS. Firstly, in section 2, an overview of different categories of MEMS and their common degradation/failure mechanisms are given. In section 3, the proposed method which aims at assessing the health state of MEMS and estimating their RUL is introduced. In addition, the description, modeling of an electrostatic micro-gripper and the results of accelerated life tests are provided in section 4. From the obtained experiments, an empirical model of the microgripper degradation is learned. This model is then combined with the analytical behavior model of the microgripper to assess its health state and estimate its RUL. Finally, a conclusion is given in section 5.

2. OVERVIEW OF MEMS AND THEIR FAILURE MECHANISMS

MEMS are introduced in 1989 when Professor Howe (Howe, 1989) from university of California at Berkeley first used the acronym to describe the hybrid use of microelectronics and mechanical components to piezo-actuate and create electrical signals. A MEMS is a system that integrates several mechanical, optical, thermal and fluidic elements using electricity as an energy source in order to perform measurement and / or actuating functions in structures having micrometric dimensions. MEMS devices have the ability to sense, control and actuate on the micro scale, and generate effects on the macro scale. They can be grouped in four main categories (D. Tanner, 2009)

- Class 1: no moving parts (pressure sensors and microphones).
- Class 2: moving parts with no rubbing or impacting surfaces (gyroscope, accelerators and RF oscillators).
- Class 3: moving parts with impacting surfaces (micromirror).
- Class 4: moving parts with impacting and rubbing surfaces (micro-motors).

MEMS technology has grown from laboratory research projects to global commercialization (Walraven, 2005) and thanks to their miniaturization, low power consumption and tight integration with control and sense electronics (Shea, 2006), MEMS are more and more utilized in numerous applications as shown in Table 1.

Categories	Examples
Micro-sensors	Pressure sensors, accelerometers, gyroscopes, thermal sensors, optical sensors, micro-bolometers, magnetometer, and microphones.
Micro-actuators	Electrostatic, piezoelectric, thermal, magnetic.
RF MEMS	Metal contact switches, tunable capacitors, tunable filters, RF switches, micro-resonators.
Optical MEMS	micro-mirrors, optical switches, Optical reflectors, attenuators.
Fluidic MEMS	Pumps, valves.
Bio MEMS	DNA chips, microsurgical instruments, intra-vascular devices, mchip, microfluidic chips.

Table 1. MEMS applications and examples.

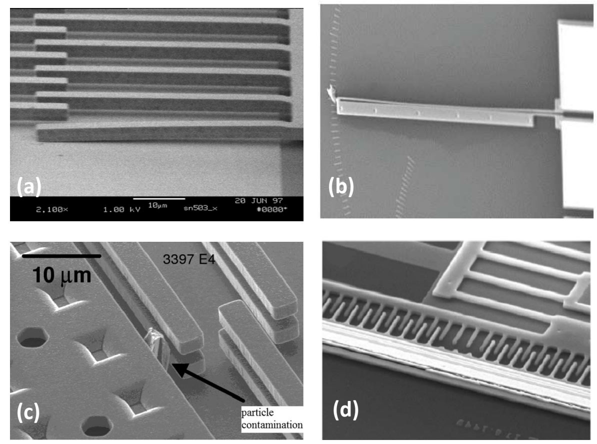

Figure 1. Failure mechanisms illustration: (a) stiction of the finger on the substrate, (b) stiction in electrothermal actuator, (c) contamination in a comb-drive, and (d) finger fracture (D. M. Tanner et al., 2000), (Dardalhon, 2003), (Mir, Rufer, & Dhayni, 2006)

Most of MEMS are designed with some basic parts such as cantilever beams, membranes, springs, hinges, etc (Merlijn van Spengen, 2003). These parts are subject to degradation and failure mechanisms due to several influence factors (temperature, humidity, vibration, noise, etc). Common failure mechanisms identified and known until now concern stiction, wear, fracture, creep, delamination, contamination, adhesion, fatigue, degradation of dielectrics, and electrostatic discharge (D. Tanner, 2009), (Merlijn van Spengen, 2003), (Shea, 2006), (McMahon & Jones, 2012), (Matmat, 2010), (Huang, Vasan, Doraiswami, Osterman, & Pecht, 2012), (Zaghloul et al., 2011), (Li & Jiang, 2008). Figure 1 shows some of these failure mechanisms.

MEMS failure modes can be classified according to two strategies: they can be categorized as failures related to manufacturing or to utilization (Matmat, 2010), or as mechanical, electrical and material based failures (Shea, 2006), (McMahon & Jones, 2012), (Ruan et al., 2009), (Müller-Fiedler, Wagner, & Bernhard, 2002). The two classifications are shown in Tables 2 and 3 .

3. PROPOSED METHOD

The main steps of the proposed method are summarized in Figure 2.
This method can be applied to different categories of MEMS, it aims at combining both degradation and nominal behavior models in order to detect and diagnose faults, estimate their health state and predict their RUL. The degradation model is obtained experimentally through accelerated life tests ((Ruan et al., 2009), (Shea, 2006)) and the nominal behavior model is derived by writing the corresponding physical equations.

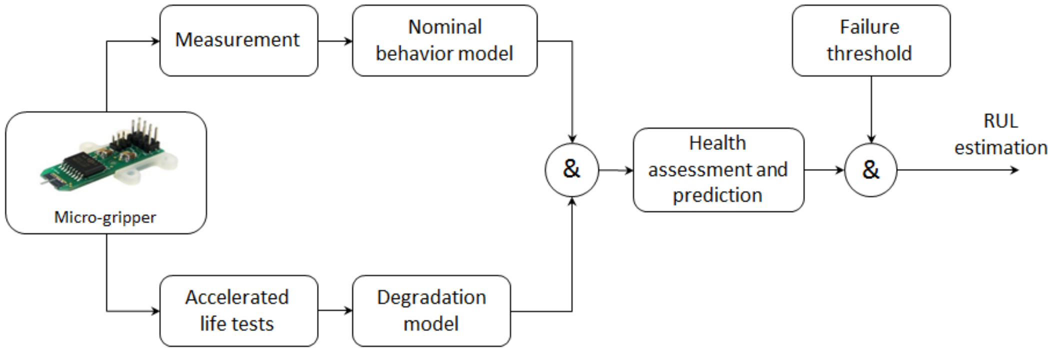

Figure 2. Main steps of the proposed hybrid prognostic method.

Mechanical	Electrical	Material
Delamination	Degradation of dielectrics	Stiction
Fracture	Electrostatic discharge ESD	Contamination
Fatigue	Electro-migration	
Creep	Electrical short circuit	
Wear	Electrical stiction	
Stiction		
Plastic deformation		
Adhesion		

Table 2. Mechanical, electrical and material based failure modes.

The estimated health state which can be represented by the parameter values is compared to the failure threshold which is obtained experimentally by observing the response of the MEMS when performing accelerated life tests to calculate the RUL. As shown in Figure 3, the RUL value corresponds to the difference between the failure time and the current time.

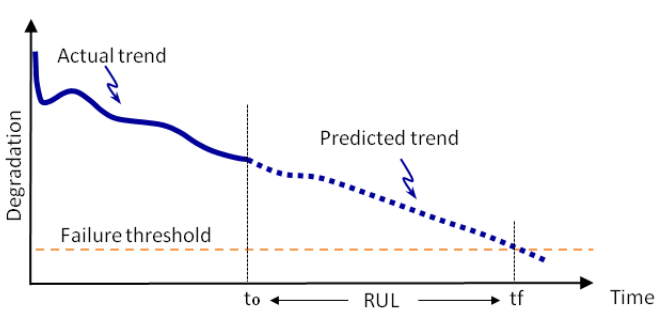

Figure 3. RUL estimation.

Related to utilization	Related to manufacturing
Stiction	Stiction
Delamination	Contamination
Fatigue	Fracture
Creep	Electrical short circuit
Wear	
Electro-migration, ESD	
Adhesion	
Electrical short circuit	
Fracture	

Table 3. Failure modes related to manufacturing or to utilization.

4. EXPERIMENTAL SETUP AND RESULTS

4.1. Description of the experiments

The experimental platform designed to perform accelerated life tests of three microgripper MEMS is shown in Figure 4. The microgripper FT-G100 used in this application and shown

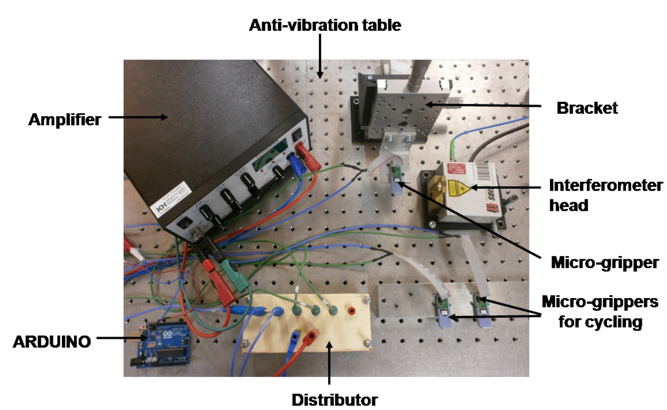

Figure 4. Overview of the experimental platform.

in Figure 5 is designed by the Swiss company Femtotools based in Zurich. The main feature of the FT-G100 is the manipulation of micro and nano objects with two arms (the first is moving, the second is static). The initial opening of the two arms is 100 μm and can be controlled with nanometer precision. The maximum actuation voltage of the microgripper is 200 V. This device consists of two mechanisms: an electrostatic actuation mechanism containing a comb-drive actuator and an actuated finger. In addition, a sensory mechanism comprises a capacitive force sensor. The comb-drive actuator contains 1300 electrodes: 650 moving electrodes and 650 static electrodes. The shuttle is the moving part of the actuator. The capacitive sensor consists of 400 electrodes.

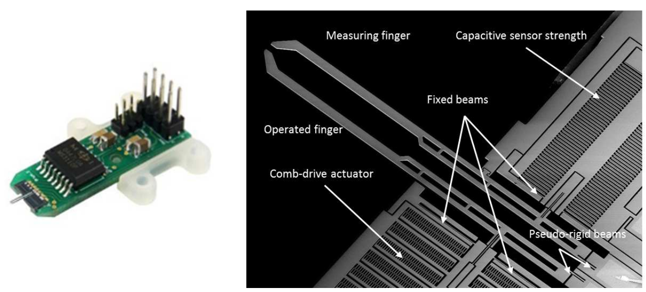

Figure 5. Microgripper FT-G100 used in the accelerated life tests.

In response to a voltage V_{in} applied to the comb-drive actuator, an electrostatic force F_{elec} is generated. This force is proportional to the square of the input voltage and its analytical expression is given by Eq. (1):

$$F_{elec} = \frac{N_a.e.h_z}{2.g}.V_{in}^2 \tag{1}$$

where $N_a = 1300$ is the number of electrodes in the comb-dive, $e = 8.85\ pF/m$ is the air permittivity, $h_z = 50\ \mu m$ is the thickness of the electrodes and $g = 6\ \mu m$ is the gap between the fixed and the mobile electrodes.

The platform is constituted of a voltage source (an ARDUINO device which generates a square signal of 5 V magnitude and frequency equal to 25 Hz), a voltage amplifier, a distributor for supplying the voltage to the three microgrippers, an interferometer and a micrometric adjustment support to fix the MEMS when taking measurements. The acquisition of measurements is the same for the three microgrippers and for each one of them the following steps are applied: (a) fix the microgripper on the support, (b) adjust the interferometer reflection (50 % minimum), (c) the reflected signal is acquired at a frequency equal to 25 kHz, with 16384 points, (d) store the result in different files in a dedicated computer for later use.

4.2. Physics-based model and parameters identification

The time response obtained experimentally from a new microgripper is shown in Figure 6. It corresponds to a second order dynamic system. The microgripper can then be modeled as a mass-spring-damper (MSD) system.

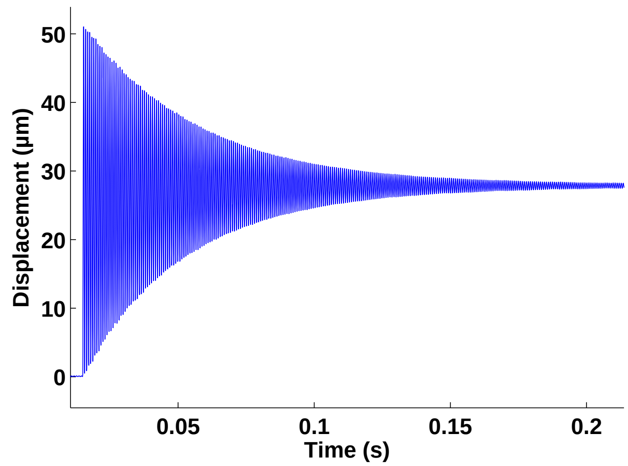

Figure 6. Time response of a new microgripper.

The governing equation of such a system is given in Eq. (2).

$$F_{elec} = M\ddot{x} + f\dot{x} + kx \tag{2}$$

where F_{elec} is the electrical force actuating the mobile arm, x is the displacement, f is the friction coefficient, k is the stiffness of the arm and M is its mass. By applying the Laplace transform on Eq.(2) and by putting $U(t) = V_{in}^2(t)$, one gets the canonical transfer function given in Eq.(3):

$$H(p) = \frac{X(p)}{U(p)} = \frac{\frac{\eta}{k}}{1 + \frac{f}{k}p + \frac{M}{k}p^2} = \frac{K}{1 + \frac{2\xi}{w_n}p + \frac{1}{w_n^2}p^2} \tag{3}$$

In Eq. (3), $K = \frac{\eta}{k}$ is the static gain of the microgripper, $w_n = \sqrt{\frac{k}{M}}$ its natural frequency and $\xi = \frac{f}{2.\sqrt{k.M}}$ its damping coefficient.

According to Eq. (3), the parameters which can vary are the natural frequency w_n, the friction coefficient f and the stiffness k. The variation of the two first parameters depends on k which can vary significantly due to cycling. In the next subsections, and in order to study the degradation of the MEMS, only the variation of its stiffness will be studied.

4.3. Experimental results

This subsection is devoted to the presentation of experimental results, the degradation model and RUL estimation.

The experiment remained running for more than two months. During the accelerated life tests, the measurements were performed every 2 160 000 cycles and at each measurement the value of the stiffness k is estimated from the time response of the corresponding microgripper. At the end of each accelerated life test, which duration is more than 140 million cycles, the evolution of the stiffness k is plotted as a function of number of cycles as shown in Figure 7.

The experimental measurements are performed for three microgrippers in the same conditions to ensure the repeatability of the parameter k. The first 20 million cycles are considered as a transient phase (interesting to study for infant mortalities but is not considered here for the prediction of RUL) and can be neglected in the model identification. Figure 7 shows the low standard deviation between the values of the stiffness k of the three microgrippers.

Before starting the identification of the degradation model, the averages of k are plotted as a function of number of cycles as shown in Figure 8.

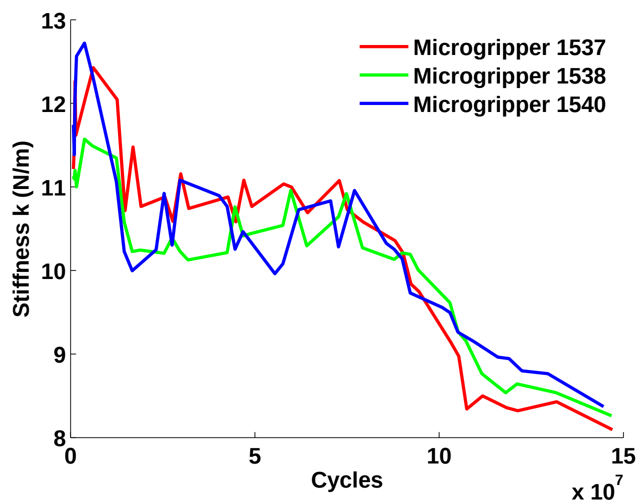

Figure 7. Experimental results.

4.3.1. Degradation model

The experimental measurements are approximated by a sixth order polynomial which better represents the shape and gives more accurate as shown in Figure 8. The mathematical equation of the green curve is estimated by using Matlab (Eq. 4).

$$k(n) = \sum_{i=0}^{6} (a_i.n^i) \tag{4}$$

where k is the stiffness, a_i the constants of the approximated polynomial (Table 4) and n is the number of cycles.

Equation (4) represents the polynomial degradation model of the microgripper. This model will be used in the next subsection to estimate the RUL.

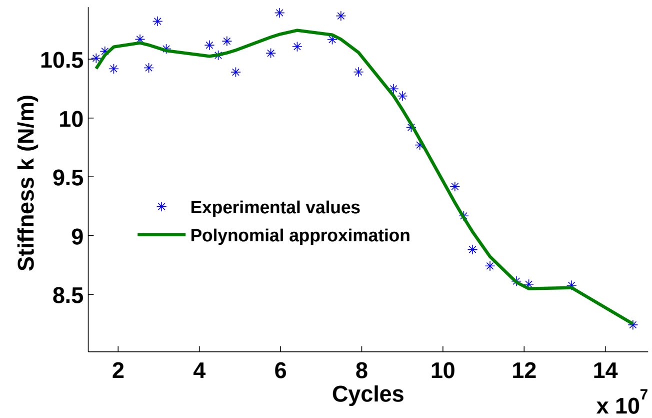

Figure 8. Six order polynomial approximation.

i	a_i	i	a_i
0	7.18	**4**	-6.03×10^{-30}
1	4.55×10^{-7}	**5**	3.35×10^{-38}
2	-2.24×10^{-4}	**6**	-7.12×10^{-47}
3	5.02×10^{-22}		

Table 4. Numerical values of the polynomial coefficients.

4.3.2. RUL results and discussion

The polynomial degradation model obtained experimentally through accelerated life tests is combined with the nominal behavior model of the microgripper in order to monitor its health state and estimate its future state. The time responses shown in Figure 9(a) are given by injecting the number of cycles in the nominal behavior model. The parameters of the system such as the settling time, the static gain, the natural frequency and the damping coefficient can be estimated. To assess the health state of the MEMS, only the settling time t_s is studied. Table 5 shows the values of k and t_s for different number of cycles n. The settling time is estimated from the time responses (Figure 9(a)) and is plotted as a function of number of cycles as shown in Figure 9(b).

$n(10^6)$	$k(N/m)$	$t_s(s)$
70	10.7367	0.102
100	9.4625	0.106
130	8.3890	0.109
150	7.8573	0.111

Table 5. Stiffness and settling time values.

The failure time T_f is obtained by fixing a settling time limit, which corresponds in this application to 150 million cycles. The RUL is then calculated as the difference between T_f and the current time t (Eq. 5). Figure 10 shows the stochastic estimation of RUL.

$$RUL = T_f - t \tag{5}$$

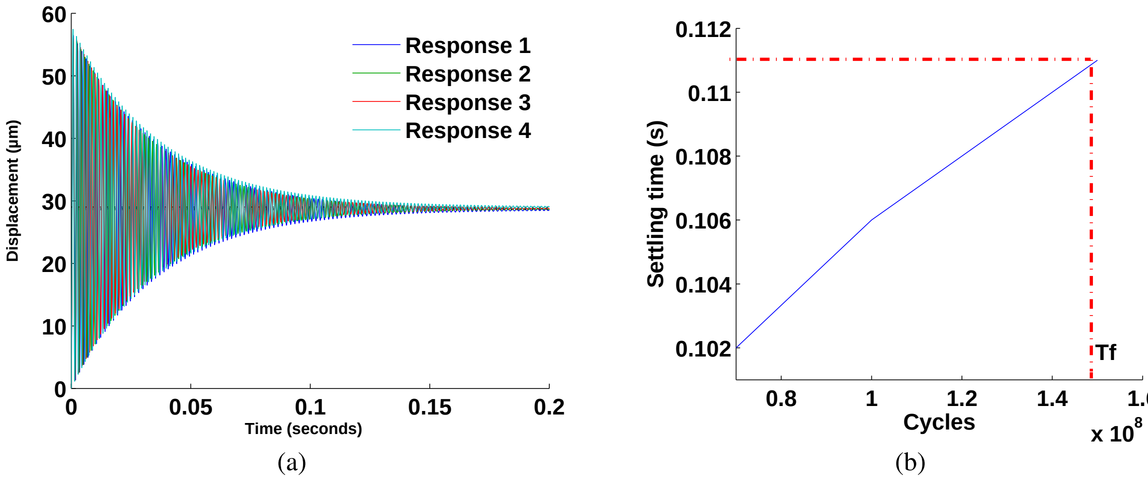

Figure 9. Time response for different values of k and settling time variation.

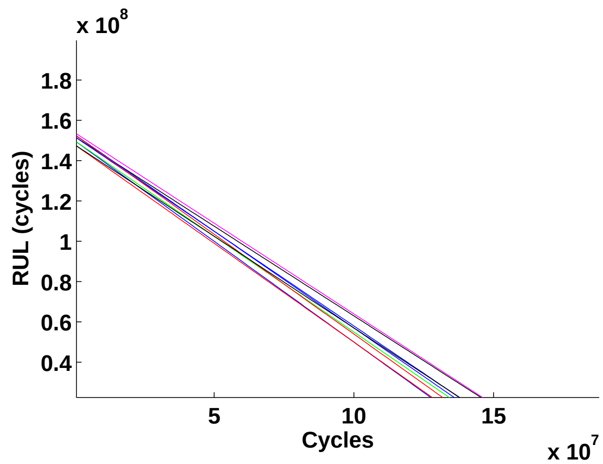

Figure 10. RUL estimation.

5. CONCLUSION

In this paper, a hybrid prognostic method of microgripper MEMS has been proposed. It is based on the combination of two models: an analytical behavior model obtained by writing the physical equations and a degradation model derived from accelerated life tests. The method is applied to assess the health state of the MEMS and estimate its RUL. By injecting the degradation model in the nominal behavior model, the time response is given and its parameters can be estimated. The latter information are then used to assess the health state of the MEMS, define a failure threshold and calculate the RUL.

The proposed method has been applied on a set of only three MEMS with constant operating conditions. It can be improved by performing experiments with more MEMS and varying the influence factors (temperature, humidity, vibration, etc) to have a degradation model which can be more representative, reliable and accurate.

REFERENCES

Aiwina, H., Sheng, Z., Andy, C. T., C, & Joseph, M. (2009). Rotating machinery prognostics: State of the art, challenges and opportunities. *Mechanical Systems and Signal Processing*, *23*, 724-739.

Dardalhon, M. (2003). *Contribution à l'analyse de la fiabilité de microsystèmes: prise en compte des contraintes liées à l'environnement spatial*. Unpublished doctoral dissertation, Montpellier 2, Université des Sciences et Techniques du Languedoc.

Hansen, J., R, Hall, L. S., D, & Kurtz, K. (1995). New approach to the challenge of machinery prognostics.

Journal of Engineering for Gas Turbines and Power, *117*, 320-325.

Howe, R. T. (1989). Microsensor and microactuator applications of thin films. *Thin Solid Films*, *181*, 235-243.

Huang, Y., Vasan, A. S. S., Doraiswami, R., Osterman, M., & Pecht, M. (2012). Mems reliability review. *Device and Materials Reliability, IEEE Transactions on*, *12*, 482-493.

Jay, L., Fangji, W., Wenyu, Z., Masoud, G., Linxia, L., & David, S. (2014). Prognostics and health management design for rotary machinery systems reviews, methodology and applications. *Mechanical Systems and Signal Processing*, *42*, 314-334.

Li, Y., & Jiang, Z. (2008). An overview of reliability and failure mode analysis of microelectromechanical systems (mems). In *Handbook of performability engineering* (p. 953-966).

Matmat, M. (2010). *Pour une approche complète de l'évaluation de fiabilité dans les microsystèmes*. Unpublished doctoral dissertation, INSA de Toulouse.

McMahon, M., & Jones, J. (2012). A methodology for accelerated testing by mechanical actuation of mems devices. *Microelectronics Reliability*, *52*, 1382-1388.

Medjaher, K., Tobon-Mejia, D. A., & Zerhouni, N. (2012). Remaining useful life estimation of critical components with application to bearings. *Reliability, IEEE Transactions on*, *61*, 292-302.

Merlijn van Spengen, W. (2003). Mems reliability from a failure mechanisms perspective. *Microelectronics Reliability*, *43*, 1049-1060.

Mir, S., Rufer, L., & Dhayni, A. (2006). Built-in-self-test techniques for mems. *Microelectronics journal*, *37*, 1591-1597.

Müller-Fiedler, R., Wagner, U., & Bernhard, W. (2002). Reliability of mems-a methodical approach. *Microelectronics Reliability*, *42*, 1771-1776.

Ruan, J., Nolhier, N., Papaioannou, G., Trémouilles, D., Puyal, V., Villeneuve, C., ... Plana, R. (2009). Accelerated lifetime test of rf-mems switches under esd stress. *Microelectronics Reliability*, *49*, 1256–1259.

Shea, H. R. (2006). Reliability of mems for space applications. In *Moems-mems 2006 micro and nanofabrication.*

Tanner, D. (2009). Mems reliability: Where are we now? *Microelectronics reliability*, *49*, 937-940.

Tanner, D. M., Smith, N. F., Irwin, L. W., Eaton, W. P., Helgesen, K., Clement, J., ... others (2000). Mems reliability: infrastructure, test structures, experiments, and failure modes. *SANDIA report*, 155–157.

Walraven, J. A. (2005). Failure analysis issues in microelectromechanical systems (mems). *Microelectronics Reliability*, *45*, 1750-1757.

Zaghloul, U., Papaioannou, G., Bhushan, B., Coccetti, F., Pons, P., & Plana, R. (2011). On the reliability of electrostatic nems/mems devices: Review of present knowledge on the dielectric charging and stiction failure mechanisms and novel characterization methodologies. *Microelectronics Reliability*, *51*, 1810-1818.